SLAC-PUB-15878

Generalized Representation of Electric Fields in Sheet Beam Klystron Gaps

A. Jensen, M. Fazio, J. Neilson and G. Scheitrum

***Abstract*—H. Kosmahl and G. Branch's derivation for the electric field in a round beam gap is closely followed to derive the electric field for a sheet beam klystron gap. The wider of the two transverse dimensions of the gap is taken to be infinite in extent and the field is derived based on an approximation of the gap field at the drift tube edge. The electric field equations are generalized using a Fourier series representation of the gap field at the drift tube edge. The analytic results are compared with numerical computations.**

***Index Terms*—Cavity, Klystron, Sheet Beam, Electric Field**

I. Introduction

SHEET beam devices are a new class of microwave tube that have the potential to compete with multi-beam devices. Like multi-beam devices, sheet beam devices have lower current density beams and increased surface area, making them particularly suited for high power applications. Reduced cathode loading increases lifetime and lower current density beams require lower magnetic fields for focusing. Sheet beam devices require only one beam, cathode, and anode. This reduced complexity may lead to several advantages over multi-beam devices, including, fewer parts, simplified manufacturing, reduced cost, increased lifetime, and greater yield.

Analytic expression for the electromagnetic fields in sheet beam gaps may help advance sheet beam technology but have not been published. Analytic expressions for the electromagnetic fields in a cylindrical gap were derived in general form by [1] and were originally derived over a half a century ago by [2]. These equations helped develop higher power klystrons in which the grid was eliminated to prevent heat dissipation problems due to electron bombardment. The field equations helped provide answers to questions about beam-gap energy exchange, gap-gap interaction, coupling, and other processes. In analogy, moving from cylindrical beams to sheet beams enables higher energy devices to be developed, but at the same time introduces many new questions and areas for research.

Questions that arise about sheet beam gaps and the differences between sheet beam gaps and cylindrical gaps include:

(1) Does RF defocusing of the beam in the interaction region have a greater effect in sheet beam gaps and if so how might it be reduced?

(2) How do velocity modulation and energy interchange between the beam and gap differ between cylindrical and sheet beam gaps?

(3) How does the extent of the electric field in the longitudinal direction compare with that of a cylindrical gap and what is the effect on coupling and gap to gap interaction?

(4) How can the low interaction impedance in sheet beam gaps be improved?

The following analysis gives a starting point for these questions and extends [1] and [2] to sheet beam devices.

Fig. 1 presents the schematic to be used for the following derivation. The gap length is *2l*. The x dimension is taken to be infinite in extent and the drift tube height is *a*.

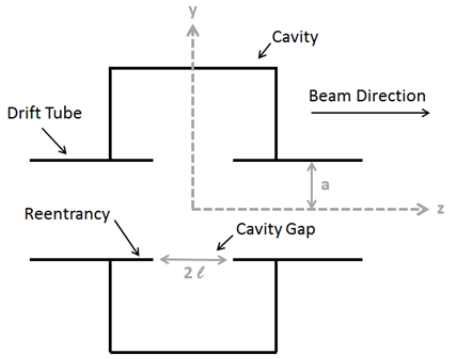

Fig. 1. Resonant klystron cavity and drift tube.

II. General Field Equations

Beginning with the wave equation,

$$\nabla^2 \vec{\mathbf{E}} = \frac{1}{c^2}\frac{\partial^2 \vec{\mathbf{E}}}{\partial t^2} \tag{1}$$

Let the x dimension of the cavity extend infinitely in x such that $E_x = 0$. The wave equation becomes,

$$\nabla^2 (E_y \hat{\mathbf{y}} + E_z \hat{\mathbf{z}}) = \frac{1}{c^2}\frac{\partial^2}{\partial t^2}(E_y \hat{\mathbf{y}} + E_z \hat{\mathbf{z}}) \tag{2}$$

Using the method of separation of variables, where $E_z(y,z) = Y(y)Z(z)$, (2) can be used to derive,

SLAC National Accelerator Laboratory, 2575 Sand Hill Road, Menlo Park, CA 94025

Work supported in part by US Department of Energy under contract DE-AC02-76SF00515.

$$\underbrace{\frac{1}{Y(y)}\frac{\partial^2}{\partial y^2}Y(y)}_{\gamma^2}+\underbrace{\frac{1}{Z(z)}\frac{\partial^2}{\partial z^2}Z(z)}_{-\beta^2}=-k^2 \tag{3}$$

where *k* is the angular wave number. Solving for Y(y),

$$\frac{1}{Y(y)}\frac{\partial^2}{\partial y^2}Y(y)=\boxed{\beta^2-k^2=\gamma^2} \tag{4}$$

gives,

$$Y(y)=A_1e^{\gamma y}+B_1e^{-\gamma y} \tag{5}$$

Since E_z is symmetric about y=0, $A_1=B_1$ and,

$$Y(y)=A_1(e^{\gamma y}+e^{-\gamma y}) \tag{6}$$

Solving for Z(z) from (3),

$$\frac{1}{Z(z)}\frac{\partial^2}{\partial z^2}Z(z)=-\beta^2 \tag{7}$$

gives,

$$Z(z)=A_2\exp(i\beta z)+B_2\exp(-i\beta z) \tag{8}$$

Let E(y,z) be defined such that if it has a propagating component, it is in the +z direction,

$$Z(z)=B_2\exp(-i\beta z) \tag{9}$$

Combining (6) and (9),

$$E_z(y,z)=\int_{-\infty}^{\infty}A(\beta)\cosh(\gamma y)\exp(-i\beta z)\,d\beta \tag{10}$$

Recognizing the Fourier form of (10) and evaluating it at y=a,

$$A(\beta)\cosh(\gamma a)=\frac{1}{2\pi}\int_{-\infty}^{\infty}E_z(a,z)\exp(i\beta z)\,dz \tag{11}$$

Let,

$$E_z(a,z)=E_0f(z) \tag{12}$$

Where f(z) is the normalized field distribution at y=a and E_o is the amplitude.

Then (11) may be written,

$$A(\beta)\cosh(\gamma a)=E_0\frac{1}{2\pi}\int_{-\infty}^{\infty}f(z)\exp(i\beta z)\,dz \tag{13}$$

Let,

$$\boxed{g(\beta)=\frac{1}{2\pi}\int_{-\infty}^{\infty}f(z)\exp(i\beta z)\,dz} \tag{14}$$

Then,

$$A(\beta)=E_0\frac{g(\beta)}{\cosh(\gamma a)} \tag{15}$$

Substituting (15) into (10),

$$\boxed{E_z(y,z)=E_0\int_{-\infty}^{\infty}\frac{\cosh(\gamma y)}{\cosh(\gamma a)}g(\beta)\exp(-i\beta z)\,d\beta} \tag{16}$$

E_y may be found from the divergence equation $\nabla\cdot\mathbf{E}=0$,

$$\boxed{\frac{\partial E_y}{\partial y}+\frac{\partial E_z}{\partial z}=0\ \Rightarrow\ E_y=-\int_0^y\frac{\partial E_z}{\partial z}dy} \tag{17}$$

Therefore,

$$\boxed{E_y(y,z)=iE_0\int_{-\infty}^{\infty}\frac{\beta}{\gamma}\frac{\sinh(\gamma y)}{\cosh(\gamma a)}g(\beta)\exp(-i\beta z)\,d\beta} \tag{18}$$

If the normalized field profile at y=a, f(z), is given, equations (14), (16) and (18) may be used to calculate the field at any value of y and z if E_z is symmetric in y about the y=0 plane and the region between y=a and y=-a is free space.

III. Knife Edge Field Approximation

Equations (18) and (16) can be solved analytically for many field profiles at y=a**.** A particularly useful field profile, is that of a knife edge gap, which may be approximated as [1], where m is a curve fitting parameter,

$$f(z)=\begin{cases}\cosh(mz) & -l<z<l\\ 0 & otherwise\end{cases} \tag{19}$$

Evaluating (14) and (19),

$$\begin{aligned}g(\beta)&=\frac{1}{2\pi}\int_{-l}^{l}\frac{\exp(mz)+\exp(-mz)}{2}\exp(i\beta z)dz\\&=\frac{1}{4\pi}\left[\frac{\exp[(i\beta+m)l]-\exp[-(i\beta+m)l]}{i\beta+m}\right.\\&\quad\left.+\frac{\exp[(i\beta-m)l]-\exp[-(i\beta-m)l]}{i\beta-m}\right]\end{aligned} \tag{20}$$

Substituting (20) into (16), (16) can be rewritten

$$
\begin{aligned}
E_z(y,z) = E_0 \Bigg\{ & \frac{\exp(ml)}{4\pi} \int_{-\infty}^{\infty} \frac{\cosh(\gamma y)}{\cosh(\gamma a)} \left[\frac{\exp[i\beta(l-z)]}{i\beta + m} \right] d\beta \\
& - \frac{\exp(-ml)}{4\pi} \int_{-\infty}^{\infty} \frac{\cosh(\gamma y)}{\cosh(\gamma a)} \left[\frac{\exp[-i\beta(l+z)]}{i\beta + m} \right] d\beta \\
& + \frac{\exp(-ml)}{4\pi} \int_{-\infty}^{\infty} \frac{\cosh(\gamma y)}{\cosh(\gamma a)} \left[\frac{\exp[\ i\beta(l-z)]}{i\beta - m} \right] d\beta \\
& - \frac{\exp(\ ml)}{4\pi} \int_{-\infty}^{\infty} \frac{\cosh(\gamma y)}{\cosh(\gamma a)} \left[\frac{\exp[-i\beta(l+z)]}{i\beta - m} \right] d\beta \Bigg\}
\end{aligned} \tag{21}
$$

Each integral may be evaluated using the residue theorem of contour integration,

$$
\int = 2\pi i \sum residues = 2\pi i \sum_{n=1}^{\#\,poles} \left. \frac{N}{D_n'} \right|_{pole_n} \tag{22}
$$

Which states that the integral around a closed loop is equal to 2πi times the sum of the residues enclosed by the loop**.** Two closed loops of integration prove useful for integrating equation (21). If $x = i\beta$, the first is from x=-i∞ to x=i∞ and then along a path of infinite radius in the left half plane. The second is the same except in the right half plane. The integration paths are shown in Fig. 2. These two integration paths are interesting, because for a given integral, the integral along the portion of the path at infinite radius goes to zero [2]. This means the integral around the closed paths are equal to the integrals in (21). To evaluate (21) the residues in the left half plane and the right half plane need to be calculated.

The residues may be calculated from equation (22) which states (for poles of order one) that the residue of the integrand associated with pole$_n$ is some numerator divided by the derivative of some denominator evaluated at pole$_n$. The numerator is the regular portion of the integrand and the denominator is the portion of the integrand that has a simple zero at pole$_n$.

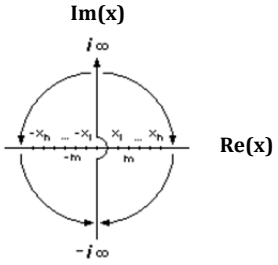

Fig. 2. Contour integration plane and poles.

Equation (21) has poles at $x = \pm m$ and $x = \pm x_n$ (see Fig. 2). Let R_n be the roots of cosine such that,

$$
\cos(\sqrt{k^2 + x_n^2}\,a) = \boxed{\cos(R_n) = 0} \tag{23}
$$

and,

$$
x_n a = \sqrt{R_n^2 - k^2 a^2} \tag{24}
$$

If x_n is to be real $ka < R_n$ or equivalently, $\boxed{ka < \pi/2}$.

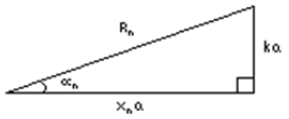

Fig. 3. Right triangle relationship between $x_n a, R_n, ka,$ and α_n.

From the relationship in Fig. 3 the variable x_n can be written,

$$
\boxed{x_n = \frac{R_n}{a}\sqrt{1 - \frac{a^2}{R_n^2}k^2} = \frac{R_n}{a}\cos(\alpha_n)} \tag{25}
$$

The framework for evaluating (21) is complete. At this point let's define L as being related to the left half plane of integration and R to the right half plane of integration.

Proceeding with the first integral in the left half plane for $z < l$,

$$
\begin{aligned}
\int_{(1L)} = \frac{\exp(ml)}{2} \Bigg[& \frac{\cos(\sqrt{k^2 + m^2}\,y)}{\cos(\sqrt{k^2 + m^2}\,a)} \exp[-m(l-z)] \\
& - \sum_{n=1}^{\infty} \frac{\cos\left(R_n \frac{y}{a}\right)}{\sin(R_n)} \frac{R_n}{a^2 x_n} \frac{\exp[-x_n(l-z)]}{x_n - m} \Bigg]
\end{aligned} \tag{26}
$$

The second integral evaluated in the right half plane for $z > -l$ is,

$$
\int_{(2R)} = -\frac{\exp(-ml)}{2} \sum_{n=1}^{\infty} \frac{\cos\left(R_n \frac{y}{a}\right)}{\sin(R_n)} \frac{R_n}{a^2 x_n} \frac{\exp[-x_n(l+z)]}{x_n + m} \tag{27}
$$

Integrating on the left half plane for $z < l$,

$$
\int_{(3L)} = -\frac{\exp(-ml)}{2} \sum_{n=1}^{\infty} \frac{\cos\left(R_n \frac{y}{a}\right)}{\sin(R_n)} \frac{R_n}{a^2 x_n} \frac{\exp[-x_n(l-z)]}{x_n + m} \tag{28}
$$

On the right half plane for $z > -l$,

$$
\begin{aligned}
\int_{(4R)} = \frac{\exp(ml)}{2} \Bigg[& \frac{\cos(\sqrt{k^2 + m^2}\,y)}{\cos(\sqrt{k^2 + m^2}\,a)} \exp[-m(l+z)] \\
& - \sum_{n=1}^{\infty} \frac{\cos\left(R_n \frac{y}{a}\right)}{\sin(R_n)} \frac{R_n}{a^2 x_n} \frac{\exp[-x_n(l+z)]}{x_n - m} \Bigg]
\end{aligned} \tag{29}
$$

Evaluating the sum of integrals for $|z| < l$

$$
\frac{E_z(y,z)}{E_0} = \int_{(1L)} + \int_{(2R)} + \int_{(3L)} + \int_{(4R)} \tag{30}
$$

$$\text{for } |z| < l$$

$$\frac{E_z(y,z)}{E_0} = \frac{\cos(\sqrt{k^2+m^2}\,y)}{\cos(\sqrt{k^2+m^2}\,a)}\cosh(mz) - \sum_{n=1}^{\infty}\frac{\cos\left(R_n\frac{y}{a}\right)}{\sin(R_n)}\frac{R_n}{a^2 x_n}\exp[-x_n l]\cdot\cosh[x_n z]\left(\frac{\exp(ml)}{x_n - m} + \frac{\exp(-ml)}{x_n + m}\right) \tag{31}$$

For $z < -l$,

$$\int_{(2L)} = -\frac{\exp(-ml)}{2}\left[\frac{\cos(\sqrt{k^2+m^2}\,y)}{\cos(\sqrt{k^2+m^2}\,a)}\exp[m(l+z)] - \sum_{n=1}^{\infty}\frac{\cos\left(R_n\frac{y}{a}\right)}{\sin(R_n)}\frac{R_n}{a^2 x_n}\frac{\exp[x_n(l+z)]}{x_n - m}\right] \tag{32}$$

For $z < -l$,

$$\int_{(4L)} = \frac{\exp(ml)}{2}\sum_{n=1}^{\infty}\frac{\cos\left(R_n\frac{y}{a}\right)}{\sin(R_n)}\frac{R_n}{a^2 x_n}\frac{\exp[x_n(l+z)]}{x_n + m} \tag{33}$$

For $z < -l$ the 2nd and 4th integrals on the opposite side are,

$$\frac{E_z(y,z)}{E_0} = \int_{(1L)} + \int_{(2L)} + \int_{(3L)} + \int_{(4L)} \tag{34}$$

Noting that $E_z(y,z) = E_z(y,-z)$,

$$\text{for } |z| > l$$

$$\frac{E_z(y,z)}{E_0} = \sum_{n=1}^{\infty}\frac{\cos\left(R_n\frac{y}{a}\right)}{\sin(R_n)}\frac{R_n}{a^2 x_n}\exp[-x_n|z|]\cdot\left(\frac{\sinh((x_n+m)l)}{x_n+m} + \frac{\sinh((x_n-m)l)}{x_n-m}\right) \tag{35}$$

E_y is calculated from (35), (31), and (17),

$$\text{for } |z| < l$$

$$\frac{E_y(y,z)}{E_0} = -\frac{\sin(\sqrt{k^2+m^2}\,y)}{\cos(\sqrt{k^2+m^2}\,a)}\frac{m\sinh(mz)}{\sqrt{k^2+m^2}} + \sum_{n=1}^{\infty}\frac{\sin\left(R_n\frac{y}{a}\right)}{a\sin(R_n)}\exp[-x_n l]\cdot\sinh[x_n z]\left(\frac{\exp(ml)}{x_n - m} + \frac{\exp(-ml)}{x_n + m}\right) \tag{36}$$

$$\text{for } |z| > l$$

$$\frac{E_y(y,z)}{E_0} = \sum_{n=1}^{\infty}\frac{z}{|z|}\frac{\sin\left(R_n\frac{y}{a}\right)}{\sin(R_n)a}\exp[-x_n|z|]\cdot\left(\frac{\sinh((x_n+m)l)}{x_n+m} + \frac{\sinh((x_n-m)l)}{x_n-m}\right) \tag{37}$$

IV. Fourier Series Field Representation

If $E_z(y,z)$ is represented as a periodic function over a period τ from $-\tau/2$ to $\tau/2$ then (16) and (18) may be written as Fourier series,

$$E_z(y,z) = E_0\sum_{n=-\infty}^{\infty}\frac{\cos(\sqrt{k^2-\beta_n^2}\,y)}{\cos(\sqrt{k^2-\beta_n^2}\,a)}g(\beta_n)\exp(-i\beta_n z) \tag{38}$$

$$E_y(y,z) = iE_0\sum_{n=-\infty}^{\infty}\frac{\beta_n}{\sqrt{k^2-\beta_n^2}}\frac{\sin(\sqrt{k^2-\beta_n^2}\,y)}{\cos(\sqrt{k^2-\beta_n^2}\,a)}g(\beta_n)\exp(-i\beta_n z) \tag{39}$$

Where,

$$\beta_n = \frac{2\pi}{\tau}n \tag{40}$$

τ is the period, and

$$g(\beta_n) = \frac{1}{\tau}\int_{-\tau/2}^{\tau/2} f(z)e^{i\beta_n x}dz \tag{41}$$

Equations (38) and (39) provide a very accurate method for calculating the electric fields. They are also useful for multi-gap cavities such as those commonly found in sheet beam klystrons for improving the R/Q or the coupling coefficient.

V. Comparison of Analytic Field Expressions and Numerical Simulations

To validate the analytic equations, simulations of a sheet beam klystron gap were done using the numerical solver Superfish. The resonant frequency of the gap was 95GHz, the gap width was 0.55mm, and *a* was 0.36mm. A least squares fit was done between the simulated result and cosh(*mz*), at y=a to find *m* (the fit was best for *m*=0.93/*l*). The simulations and equations are in good agreement and are plotted below in Fig. 4. Comparison of the Fourier series representation of the fields and simulation were also conducted but showed no noticeable discrepancies.

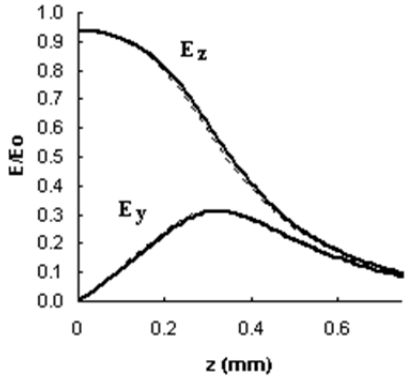

Fig. 4. Comparison of E_y and E_z at y=a/2 (Simulation – Solid Lines, cosh(mz) Approximation – Dashed Lines).

VI. Conclusion

Sheet beam devices are promising new microwave devices. Due to increased surface area, sheet beam devices are suited for high power applications and have the potential to compete with multi-beam devices. Their simple design may reduce cost, increase lifetime, and improve yield.

The electromagnetic field derivations in [1] and [2] were extended to sheet beam devices. The E_y and E_z field components for a sheet beam gap were derived assuming that the field at y=a was given and has the form $E_o\cosh(mz)$, where E_o and m were chosen to match the field using a least squares fit method. The fields were shown to have good agreement with simulations.

The field equations were generalized by approximating the field shape at y=a using a Fourier series. This provided an analytic equation that approached the simulated results as the number of terms in the Fourier series approached infinity. The Fourier series method for representing the field allows for representation of more complex fields, such as multi-gap cavities, which are commonly used in sheet beam klystrons to increase the interaction impedance or coupling coefficient.

References

[1] H. G. Kosmahl and G. M. Branch, Jr., "Generalized representation of electric fields in interaction gaps of klystrons and traveling-wave tubes," *IEEE Trans. Electron Devices,* vol. ED-20, pp. 621-629, July 1973.

[2] C. C. Wang, "Electromagnetic field inside a cylinder with a gap," *J. Appl. Phys.,* vol. 16, pp. 351-366, June 1945.